Journal of Applied Polymer Science

Simulation Study on the Liquid-Crystalline Ordering and Fluidity of Energetic Diblock Copolymers Based on Poly[3,3-Bis(azidomethyl) Oxetane]

Zhou Yang,[1,2] Long Xin-Ping,[3] Zeng Qing-Xuan[1]

[1]Institute of Chemical Materials, Chinese Academy of Engineering and Physics, Mianyang 621900, China
[2]School of Mechanical and Electrical Engineering, Beijing Institute of Technology, Beijing 100081, China
[3]Chinese Academy of Engineering and Physics, Mianyang 621900, China
Correspondence to: Z. Yang (E-mail: zhouy@caep.ac.cn)

ABSTRACT: The liquid-crystalline ordering and fluidity of energetic diblock copolymers based on poly[3,3-bis(azidomethyl) oxetane] (BAMO) and 3-nitratomethyl-3′-methyloxetane (NMMO) were investigated by the dissipative particle dynamics method. The results show that these copolymers, with moderate BAMO block lengths (x's), experienced the disorder, nematic, and smectic phases with decreasing temperature. The nematic phase was suppressed when the rod length was too long or short. After the formation of the smectic phase, the fluidity had a sharp decline. The temperature forming the smectic phase was defined as the order–disorder transition temperature (T_{ODT}) and depended strongly on x. A simple scaling rule, $T_{ODT} \approx e^{-x}$, between T_{ODT} and x was constructed. The effect of the soft NMMO block fraction on the fluidity emerged before the formation of the smectic phase. These results can help researchers design and synthesize new energetic copolymers with an appropriate melting temperature range for use as binders of solid propellants. © 2013 Wiley Periodicals, Inc. J. Appl. Polym. Sci. 129: 2772–2778, 2013

KEYWORDS: copolymers; rheology; theory and modeling

Received 16 October 2012; accepted 16 December 2012; published online 4 February 2013
DOI: 10.1002/app.38922

INTRODUCTION

Energetic polymers are of growing importance in the formulation of cast-cured composite solid propellants.[1] Common binders are generally used to bind together solid propellant ingredients in a tough elastomeric three-dimensional structure capable of absorbing and dissipating energy. Energetic binders can also increase the burning rate and specific impulse of propellant systems. This can lead to the development of a new generation of propellants. For example, oxidizers such as ammonium perchlorate can be replaced by halogen-free compounds to produce propellants with a low signature and low environmental pollution. Among them, azido polyethers, which are used as energetic binders of solid propellants and plastic-bonded explosives, have attracted great interest.[1,2] Compared with glycidyl azide polymer (GAP), one of the most thoroughly studied energetic binders, poly[3,3-bis(azidomethyl) oxetane] (BAMO) has advantages in energy output. Unfortunately, it is a crystalline polymer with a symmetric chain and cannot be used as an energetic binder through the traditional curing process at 60°C.[3] To reduce the high costs of production for azido polyethers, energetic thermoplastic elastomers have been developed.[4,5] BAMO plays an important role as the hard block in the preparation of energetic thermoplastic elastomers. Therefore, several block copolymers have been synthesized by the introduction of a soft block, such as BAMO–GAP[6,7] or BAMO–3-nitratomethyl-3′-methyloxetane (NMMO),[8,9] to prevent the crystallization of BAMO. BAMO can form physical crosslinks at predetermined temperatures due to its symmetrical side chains increasing the stiffness of the backbone; it can be cyclically used to effectively decrease the environmental problems associated with it.[4,5] In fact, propellants are always cast into a rocket motor in a conventional manner; this requires them to have good fluidity in the melt. BAMO with its rigid backbone would show liquid-crystalline behavior and could significantly influence the fluidity if the BAMO content is too high. If BAMO content is too low, energetic copolymers would lose the advantage of high energy. The optimal balance between the fluidity and the BAMO content becomes a significant problem in the design of a new generation of propellants, so researchers need to determine the fluidity of BAMO block copolymers.

Taking the energetic BAMO–NMMO diblock copolymer as an example in this study, we first investigated its liquid-crystalline

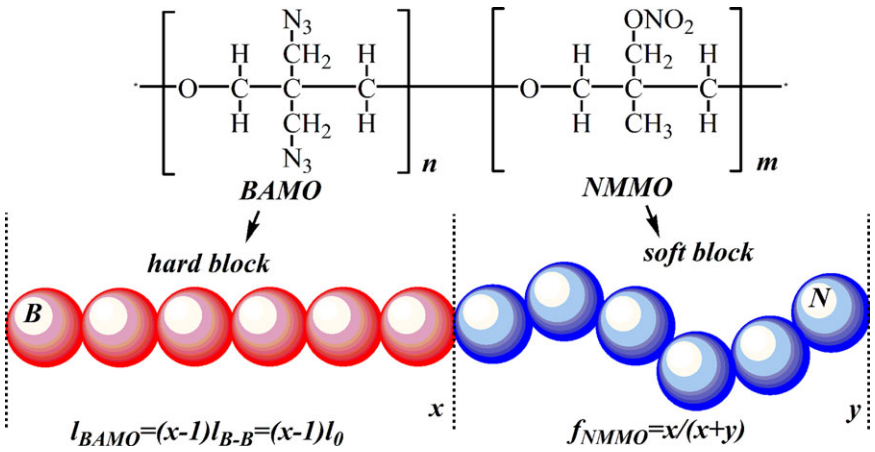

Figure 1. Molecular structures and coarse-grained models of the energetic BAMO–NMMO diblock copolymer. [Color figure can be viewed in the online issue, which is available at wileyonlinelibrary.com.]

ordering in a melt and obtained the parameters influencing its order–disorder transition temperature (T_{ODT}). It has been found in experiments,[10,11] theories,[12] and simulations[13,14] that the T_{ODT} depends strongly on the architecture of the molecule. This study mainly focused on the effect of the length and ratio of the BAMO block on the T_{ODT}. Second, we studied the influence of the liquid-crystalline behavior on the fluidity for the BAMO–NMMO diblock copolymer. Experimental studies are very expensive and dangerous for energetic materials. Recently, computer simulations[15,16] have often been used to describe the progress of the order–disorder transition for rod–coil block copolymers, especially dissipative particle dynamics (DPD) simulations.[17–20] In previous works, the DPD method has been successfully used to study the interfacial properties of GAP/HTPB blends[21] and the effect of the morphologies on the mechanical properties for the energetic GAP block copolymers.[22] In addition, a model describing the rigid block based on the angular potential in the DPD method was also constructed[23] and was used to study the influence of nanorods on the interfacial properties.[24] Therefore, we chose the DPD method to study the previous two problems.

SIMULATION DETAILS

The DPD method is a coarse-grained particle-based dynamics simulation technique that can correctly describe the hydrodynamics behavior.[25–27] The interaction between DPD particles can be expressed by a conservative force (F^C), a dissipative force (F^D), and a random force (F^R), respectively. The total force exerted on particle i (f_i) is given by the following equations:

$$f_i = \sum_{j \neq i} (F_{ij}^C + F_{ij}^D + F_{ij}^R) \tag{1}$$

The different parts of the three forces describing the nonbonded interaction are given by

$$\begin{aligned} F_{ij}^C &= -a_{ij} w^C(r_{ij}) e_{ij} \\ F_{ij}^D &= -\gamma w^D(r_{ij})(e_{ij} v_{ij}) e_{ij} \\ F_{ij}^R &= \sigma w^R(r_{ij}) \xi_{ij} \, \Delta \, t^{-0.5} e_{ij} \end{aligned} \tag{2}$$

where $r_{ij} = r_i - r_j$, $r_{ij} = |r_{ij}|$, $e_{ij} = r_{ij}/r_{ij}$, and $v_{ij} = v_i - v_j$. ζ_{ij} is a random number with zero mean and unit variance. α_{ij} is the maximum repulsion parameter, which reflects the chemical characteristics of the interacting particles. w^C, w^D, and w^R are three weight functions. For w^C, a simple soft potential is chosen as $w^C(r_{ij}) = 1 - r_{ij}$ for $r_{ij} < 1$ and $w^C(r_{ij}) = 0$ for $r_{ij} \geq 1$.[26] Unlike w^C, w^D and w^R have a certain relation to satisfy the fluctuation–dissipation theorem; this simultaneously requires a relation between the friction coefficient (γ) and the noise amplitude (σ) as follows:

$$w^D(r_{ij}) = [w^R(r_{ij})]^2; \; \sigma^2 = 2\gamma k_B T \tag{3}$$

where k_B is Boltzmann's constant and T is the temperature. w^D and w^R also use the same simple form as w^C. The forces describing the bonded particles are obtained by the differential of the spring and angle potential:[24]

$$\begin{aligned} F_{(i,i+1)}^S &= -\nabla U_{(i,i+1)}^S; \; U_{(i,i+1)}^S = \sum_i 1/2 k_S (l_{(i,i+1)} - l_0)^2 \\ F_{(i-1,i+1)}^A &= -\nabla U_{(i-1,i,i+1)}^A; U_{(i-1,i,i+1)}^A \\ &= \sum_i k_A [1 - \cos(\phi_{(i-1,i,i+1)} - \phi_0)] \end{aligned} \tag{4}$$

where $l_{(i,i+1)}$ is the bond length between the connected two particles i and $i+1$, $\phi_{(i-1,i,i+1)}\varphi$ is the bond angle of the adjacent threes particle $i-1$, i, and $i+1$. In DPD, the particles connected by the spring force can be used to represent the polymers. If the angle force is introduced additionally, those rod–coil block copolymers can be also described successfully. In fact, the method[23,24] that we used used was very similar to that used by Chou et al.[28] The only difference is that they mainly emphasized the function of the spring force. Therefore, the larger spring coefficients ($k_S = 100$) and a comparative small bending constant ($k_A = 20$) were used in their study.

Figure 1 gives the molecular structure and coarse-grained model for the energetic BAMO–NMMO diblock copolymer. According to the rigid backbone, the BAMO block is coarse grained to the hard (or rod) block; this is achieved through a larger bending coefficient ($k_A = 100$) and k_S ($k_S = 40$) in eq. (4). The larger k_A

Table I. Number of Particles in Each Block, l_{box}, the Ratio between l_{box} and R_g, l_{BAMO}, and the Number of Copolymers in Each Box at $\rho = 4$

	x	y	l_{box}	l_{box}/R_g	l_{box}/l_{BAMO}	Number of B_xN_y
B_xN_y	5	2, 3, 4, 5	10	8.3–11.7	7.0	571, 500, 444, 400
	10	4, 6, 8, 10	15	6.9–9.6	8.3	1205, 1055, 938, 845
	15	15	22	7.0	7.5	1067
	20	8, 12	25	6.9, 7.6	7.2	1143, 1000

can drive the angle between two consecutive bonds to be close to the value of π and provide a satisfactory rodlike formation. The larger k_S can fix the bond length ($l_0 = 0.2$). Finally, a rigid BAMO block with a fixed length (l_{BAMO}) can be obtained. l_{BAMO} is the function of the number of particle B (x; see Figure 1). Therefore, x can be used to represent l_{BAMO}. The NMMO block is coarse grained to the soft (or coil) block represented by particle N; $k_A = 0$ and $k_S = 4$ are used. The model (B_xN_y) can be mapped into the real energetic diblock copolymer on the basis of the following relationship between the Flory–Huggins parameter (χ_{ij}) and the repulsion parameter (α_{ij}) between unlike particles:[14,26] $\alpha_{ij} = \alpha_{ii} + 2.05\chi_{ij}$. The repulsion parameters between the like particles ($\alpha_{CC} = \alpha_{RR} = 20$) and the unlike particles ($\alpha_{RC} = 25$) and then the corresponding Flory–Huggins interaction parameter ($\chi_{BAMO-NMMO} \approx 2.44$) are used; this can also be calculated from the solubility parameter based on $\chi_{BAMO-NMMO} = V_{bead}(\delta_B - \delta_N)/kT$, where V_{bead} is the volume of a DPD particle and δ_B and δ_N are the solubility parameters of BAMO and NMMO, respectively. They depend on the chemical nature of species and can be obtained by the Fedors and van Krevelen methods incorporated in the SYNTHIA code (Accelrys). Our previous work showed that the computed solubility parameters for energetic polymers were in good agreement with the experimental data.[21] Here, $\delta_B = 21.3$ and $\delta_N = 18.4$ $MPa^{0.5}$; we could obtain $V_{bead} \approx 625.3$ $Å^3$; this corresponded to about five BMAO repeat units (the molar volume per repeat unit was about 123.9 $Å^3$) and six NMMO units (~101.1 $Å^3$). Therefore, the coarse-grained model B_xN_y represented the real energetic diblock copolymer $BAMO_{5x}NMMO_{6y}$ ($x = n/5$, $y = m/6$), x and y is the number of DPD particle B and N, respectively.

Table I shows the composition of the B_xN_y copolymers and the corresponding simulation boxes in this study. To prevent finite size effects, 6 × 6 × 6, 8 × 8 × 8, 9 × 9 × 9, 10 × 10 × 10, 12 × 12 × 12, and 15 × 15 × 15 simulation boxes were chosen for the B_5N_5 copolymer. The results show that the root mean square of the radius of gyration (R_g) had no obvious variation when the box length exceeded 9; this indicated that the small 9 × 9 × 9 box could effectively eliminate the finite size effect for B_5N_5. Then, the ratio of the box side length (l_{box}) to R_g was 5.6, or less than 6. Additionally, it should use a box of at least 1.5 or 2 times the rod length. Table I shows that simulation boxes used in this study could ensure a l_{box}/R_g value of greater than 6 and the smallest ratio of l_{box} to l_{BAMO} of about 7; therefore, we could effectively avoid the finite size effects of rods. Simulation boxes with periodic boundary conditions were first run at a high temperature. With this, we obtained a high-disordered initial system, which was then annealed to a lower temperature. We controlled the desired temperature by fixing γ at 2.66 and varying σ in eq. (3).[13,14] The time step $\Delta t = 0.001$ was used to eliminate the effect of the larger k_A on the system stability and to achieve better temperature control. A total of 3–5 × 10^6 DPD steps were carried out to guarantee the equilibrium of the simulation systems for all of the DPD simulations.

RESULTS AND DISCUSSION

First, the progress of liquid-crystalline ordering that can influence the fluidity of energetic B_xN_y copolymers was investigated by calculation of the order parameter (S). This was done by the evaluation of the matrix:

$$Q = \frac{1}{2}\left(3\left\langle \hat{u}_i \hat{u}_j \right\rangle - 1\right) \tag{5}$$

where $\hat{u}_i$ is the unit vector parallel to the ith rod and S is the largest (positive) eigenvalue of this matrix and runs from 0 for randomly oriented rods to 1 for perfectly oriented rods. Second, the fluidity of the energetic B_xN_y copolymers was investigated by calculation of the diffusion coefficient (D) as follows:

$$D = \frac{1}{6}\lim_{t\to\infty}\frac{d}{dt}\sum_{i=1}^{N}\left\langle |\mathbf{r}_i(t) - \mathbf{r}_i(0)|^2 \right\rangle \tag{6}$$

where $\mathbf{r}_i$ denotes the position vector of ith particle and the angular brackets denote an ensemble average. So the limiting slope of the mean square displacement as a function of time could be used to evaluate D of a particle undergoing random Brownian motion in three dimensions.

A plot for the calculated S and D values of the BAMO block in the $B_{10}N_{10}$ copolymers is shown as a function of the temperature in Figure 2. With increasing temperature, the $B_{10}N_{10}$ copolymer went through the normal three stages, that is, the disorder phase, the nematic phase, and the smectic phase. The corresponding S (or temperature) was $0 < S < 0.4$ (or $T \geq 1.7$) for the disorder phase, $0.4 \leq S < 0.9$ (or $1.4 < T < 1.7$) for the nematic phase, and $0.9 \leq S$ ($T \leq 1.4$) for the smectic phase. These findings were in good agreement with the simulation results.[13,14] We noted that the temperature with DPD units was not the corresponding real temperature. Therefore, these results can only help researchers to understand the variation tendency of physical phenomena. Figure 2 also shows that D had an approximately linear decrease when the temperature changed from 2.5 to 1.4. In this range, the $B_{10}N_{10}$ copolymer has a transition from the disorder phase to the nematic phase. Obviously, this phase transition did not evidently influence the fluidity of

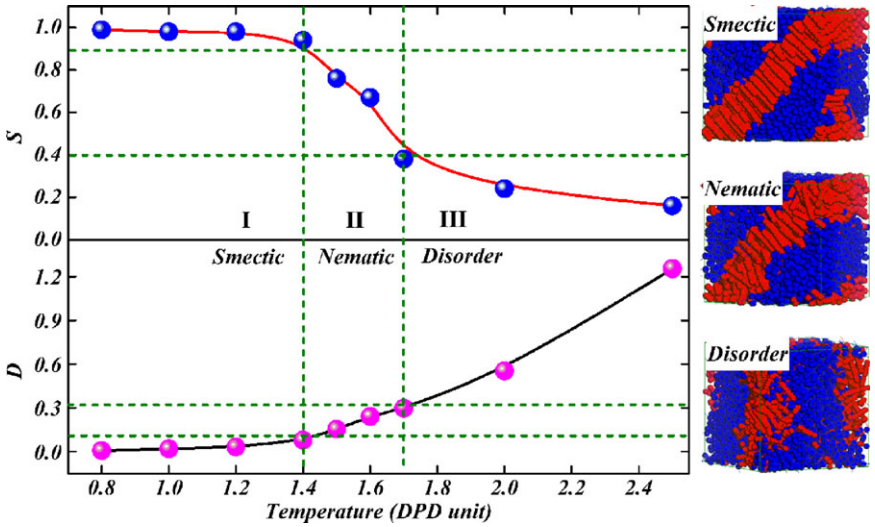

Figure 2. Snapshot of the disorder, nematic, and smectic phases and plot of S and D versus the temperature for $B_{10}N_{10}$. [Color figure can be viewed in the online issue, which is available at wileyonlinelibrary.com.]

the $B_{10}N_{10}$ block copolymer. In fact, the distinct decline (ca. one order of magnitude) of D only occurred after the transition from the nematic phase to the smectic phase at about $T = 1.4$. We could reason that the morphology of the solid $B_{10}N_{10}$ copolymer should have been very close to its smectic phase because of the very low diffusion ability.

To investigate the effect of the BAMO block length (x) on the liquid-crystalline ordering, the S and D values of the BAMO block in the B_5N_5 and $B_{15}N_{15}$ were calculated, and the results are shown in Figure 3. The x values of B_5N_5 ($x = 5$) was shorter than that of $B_{10}N_{10}$ ($x = 10$). Figure 3(a) show that the S value for B_5N_5 jumped from 0.4 to 0.9 with a decrease in the temperature; this indicated a sharp transition from the disorder phase to the smectic phase. This also indicated that the B_5N_5 energetic copolymer kept the disorder morphology in the wider range of temperature ($T \geq 0.5$, not the 1.7 of $B_{10}N_{10}$) because of its shorter x. As shown in Figure 3(a), the B_5N_5 copolymer formed a lamellar phase at $S \approx 0.4$, which was very similar to the nematic phase when the temperature was close to $T = 0.5$. The nematic phase could be regarded as a transition state during this (disorder to smectic) phase transition. In Figure 3(b), S of the $B_{15}N_{15}$ copolymer also had a sharp transition and jumped from 0.41 to 0.86. It was very similar to that of the B_5N_5 block copolymer, and the only difference was that the $B_{15}N_{15}$ copolymer kept the smectic morphology in the wider range of temperature ($T \leq 2.1$, not the 1.4 of $B_{10}N_{10}$) because of its longer x. Wilson and coworkers[18,29] found similar results. They reasoned that for a sufficiently long rigid block, the nematic phase was suppressed altogether, and a disorder–smectic phase transition could be observed. Our study showed that the diblock copolymer with a sufficiently short rigid block could also result in the same phenomenon.

As for D of the B_5N_5 copolymer, a familiar phenomenon as with the $B_{10}N_{10}$ copolymer could be found. It also showed a

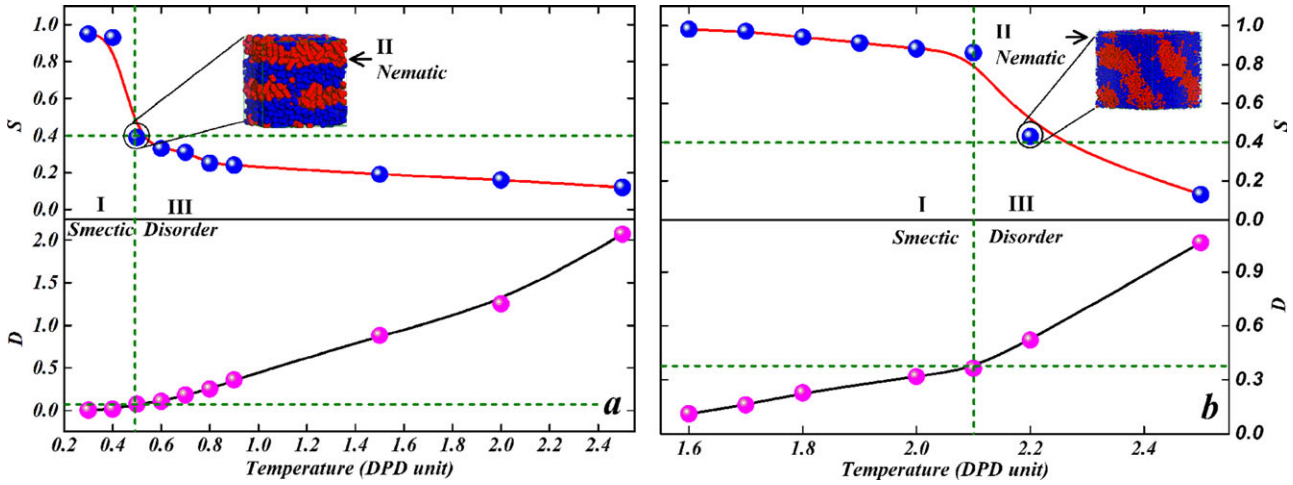

Figure 3. Plot of S and D versus the temperature for (a) B_5N_5 and (b) $B_{15}N_{15}$. [Color figure can be viewed in the online issue, which is available at wileyonlinelibrary.com.]

Applied Polymer SCIENCE

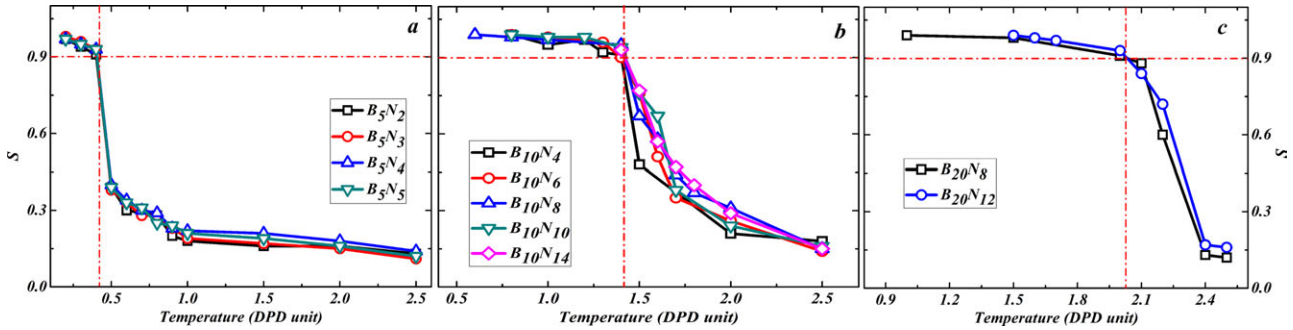

Figure 4. Plot of S as a function of temperature for (a) B_5N_y, $y = 2$, 3, 4 and 5; (b) $B_{10}N_y$, $y = 4$, 6, 8, 10 and 14; and (c) $B_{20}N_y$, $y = 8$ and 12. [Color figure can be viewed in the online issue, which is available at wileyonlinelibrary.com.]

linear decrease before the disorder–smectic phase transition. D abruptly dropped an order of magnitude after the formation of the smectic phase ($S \approx 0.9/T \approx 0.4$). D of $B_{15}N_{15}$ copolymer also had a linear decrease before the formation of the $B_{15}N_{15}$ copolymer. However, it did not show a sharp transition near the point of the disorder–smectic phase transition. The possible reason was that the $B_{15}N_{15}$ copolymer with a long rigid block could have formed the smectic phase at a higher temperature ($T \approx 2.1$). This result shows that the temperature was still the first element that determined the fluidity of the copolymer. Although there was no sharp variation, an essential decline in D of the $B_{15}N_{15}$ copolymer could still be found. This result shows that the effect of the smectic phase on the fluidity was significant and could not be neglected.

In general, energetic block copolymers are often used as typical binders of solid propellants and cast to fill in several complicated shapes. Therefore, the fluidity of the propellant binders in the melt was a key parameter. As for BAMO, it could not be used directly as a binder for solid propellants.[3] The main reason is that it has no fluid ability because of the solid phase at the casting temperature. Therefore, one needs to use soft blocks to tune the fluidity of energetic block copolymers based on BAMO. Here, the BAMO–NMMO block copolymer was chosen to analyze the influence of the NMMO segments on the fluidity. The results can help researchers to select an appropriate configuration of energetic copolymers and ensure that they have an optimal casting temperature or processing properties when they are used as propellant binders.

The previous analysis showed that the smectic phase had a significant effect on the fluidity. Therefore, the effect of the NMMO blocks on the liquid-crystalline ordering phase transition was also investigated, and the results are given in Figure 4. There was not a notable shift with increasing volume fraction of the NMMO blocks [$f_{NMMO} = y/(x + y)$] when x was fixed. For example, in Figure 4(a) ($x = 5$), the corresponding temperature of the phase transition point ($S = 0.9$) was always $T = 0.4$ when y increased from 2 to 5 ($0.28 \leq f_{NMMO} \leq 0.5$). In addition, when the x values were 10 [Figure 4(b)] and 20 [Figure 4(c)], the corresponding temperatures of the phase transition point ($S = 0.9$) were 1.4 and 2.0, respectively. They did not show obvious changes with increasing f_{NMMO}. These results only tell us that the NMMO block had no influence on the smectic phase and its corresponding temperature. However, in Figure 4(b), we observed that the NMMO block had a little influence on the process before the formation of the smectic phase. Second, the effect of the NMMO block on the fluidity of the BAMO–NMMO copolymer was investigated, and the results are given in Figure 5. In Figure 5(a), x is fixed at $x = 5$, f_{NMMO} is in the range 0.28–0.5, and the corresponding number of particles N is 2–5. Figure 5(a) shows that f_{NMMO} had a significant influence on D of the BAMO–NMMO copolymer at the stage of high temperature ($T > 0.7$) and hardly had any obvious influence when $T \leq 0.7$ [see the vertical line in Figure 5(a)]. Similar results were also found for the $B_{10}N_y$ systems shown in Figure 5(b), where in the two comparisons with B_5N_y, the divided point of temperature was about 1.2 [see the vertical line in Figure 5(b)]. Figure 5(c) shows a different result, which was that f_{NMMO} had no obvious influence on D of the $B_{20}N_y$ systems during the whole zone of temperature. The reason may have been the longer rigid BAMO block, which could result in the formation of the smectic phase at a high temperature. In the meantime, D of the BAMO–NMMO copolymer was determined by the temperature and not the smectic phase, and this was in agreement with the aforementioned.

If the energetic copolymer is used as a binder, it should have a melting temperature that falls within a desirable range (e.g., 60–120°C)[4,5] when one considers the processing and the final properties. As shown in Figure 5(a,b), only when the rigid BAMO block had an appropriate length could the fluidity of the BAMO–NMMO copolymer be tuned by f_{NMMO}. However, once the length for the rigid BAMO block exceeded a certain range, the soft NMMO block no longer influenced the fluidity [see Figure 5(c)]. From Figure 5(a), we can see that when the B_5N_y copolymer systems retained the same diffusivity in the range of $y = 2$–5, they could span a broad temperature zone denoted by the horizontal dashed dotted line with two arrows. When the systems were located at a same level of temperature, the B_5N_2 copolymer had the highest diffusivity (or fluidity), and B_5N_5 had the lowest one (see the vertical dashed dotted line with two arrows). In other words, the larger B_5N_2 had a disadvantageous effect on the processing properties of the BAMO–NMMO block copolymers. The B_5N_y copolymer systems in Figure 5(b) also showed a similar rule.

As mentioned previously, an obvious variation for the S and D values of the BAMO–NMMO block copolymers occurred at the

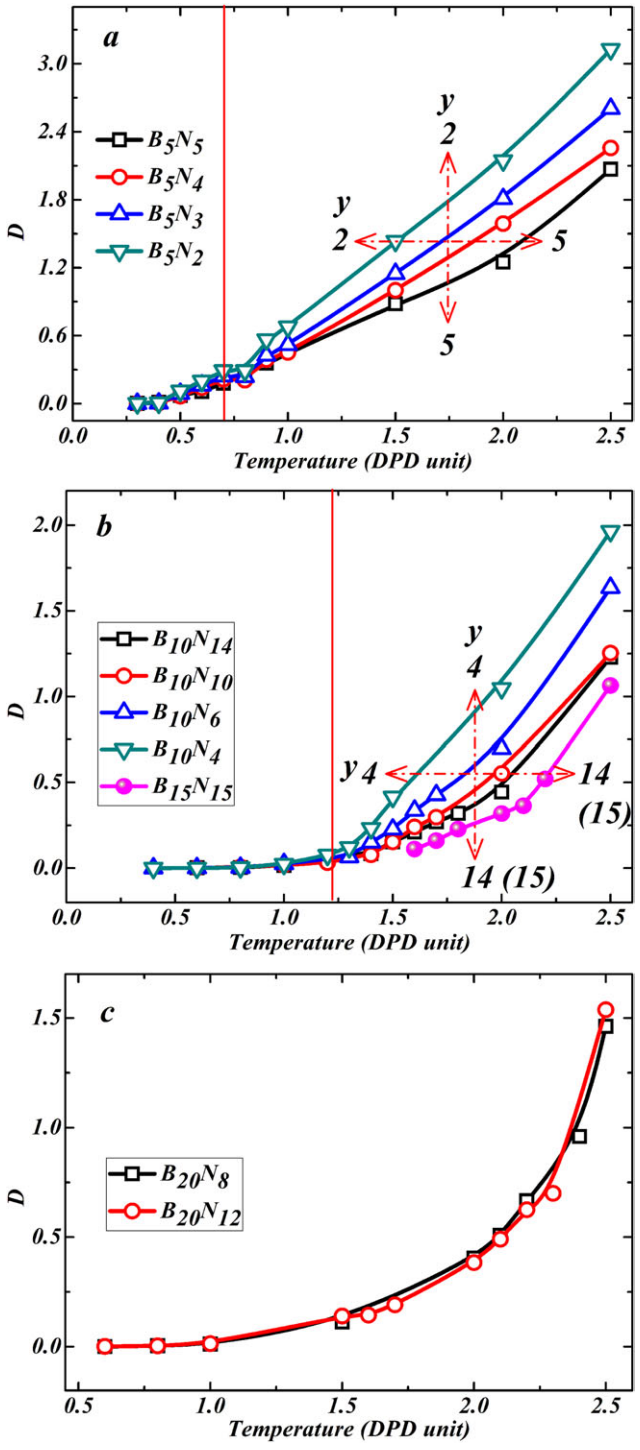

Figure 5. Plot of D as a function of temperature for (a) B_5N_y, $y = 2$, 3, 4 and 5; (b) $B_{10}N_y$, $y = 4$, 6, 10, 14 and $B_{15}N_{15}$; (c) $B_{20}N_y$, $y = 8$ and 12. [Color figure can be viewed in the online issue, which is available at wileyonlinelibrary.com.]

point $S \approx 0.9$; this also corresponded to the formation of the smectic phase. Therefore, the state after $S = 0.9$ was defined as a high-ordering phase, which included the smectic phase, and the state before $S = 0.9$ was defined as a low-ordering phase, which included the disorder and nematic phases. $S = 0.9$ as a criterion of T_{ODT} for the BAMO–NMMO block copolymers had a clearly physical meaning, which was that the BAMO–NMMO copolymers experienced a transition from a low-ordering (disorder and nematic) to a high-ordering (smectic) phase. At the same time, this transition had a significant influence on the fluidity of the BAMO–NMMO copolymers. This means that the fluidity of the BAMO–NMMO copolymers experienced a sharp variation at about $S = 0.9$. Here, the temperature corresponding to $S = 0.9$ was defined as the T_{ODT}; this was not completely consistent with a generalized temperature of T_{ODT}.

In addition, as shown in Figures 4 and 5, the defined T_{ODT} could not be influenced by f_{NMMO} and had a scaling rule with x. The detailed relationship between T_{ODT} and x is given in Figure 6; it exhibited a simple exponential form: $T_{ODT} \approx e^{-x}$. Moreover, the correlation coefficients ($R^2 = 0.999$) were all very close to 1, which confirmed the reliability for this scaling rule.

CONCLUSIONS

Energetic copolymers are generally used as binders of solid propellants and are applied via the casting method. Therefore, fluidity in the melt is a key parameter that can influence their extensive use. In this study, BAMO–NMMO diblock copolymers were used as an example, and their liquid-crystalline ordering and fluidity were studied by the dissipative particle dynamics simulation method. A basic understanding of the relationship between the liquid-crystalline ordering and the fluidity of these copolymers was determined.

The results show that with decreasing temperature, the BAMO–NMMO copolymers with a moderate rigid x went through three stages, that is, the disorder, nematic, and smectic phases. The nematic phase was suppressed when x was too long or short. The BAMO–NMMO copolymers at every stage had different fluidities (as monitored by D). After the formation of the smectic phase, D had a sharp decline when the BAMO–NMMO copolymers had low and moderate x values. However, for the BAMO–NMMO copolymers with long x values, they always had

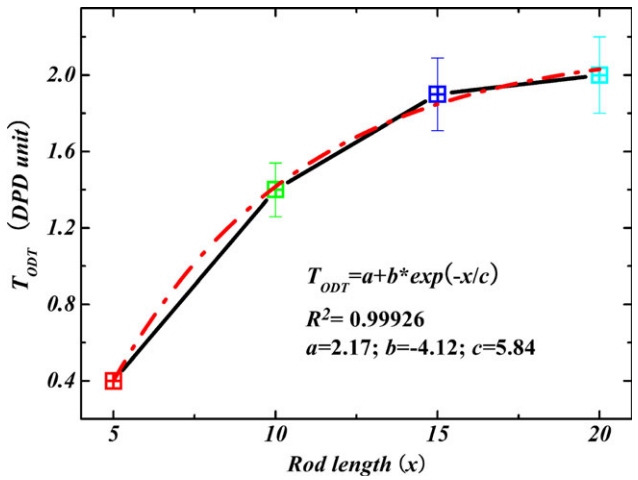

Figure 6. Relation between T_{ODT} and x; the dash dot line is the fitting result. [Color figure can be viewed in the online issue, which is available at wileyonlinelibrary.com.]

a higher D even when they formed the smectic phase. The reason was that their temperatures forming the smectic phase were far greater than the others with the low and moderate ones. Therefore, the temperature was still the most important parameter determining the fluidity of the rod–coil copolymers.

The temperature of the arising smectic phase ($S = 0.9$) was defined as T_{ODT} and depended strongly on the rigid x. An influence of the soft NMMO block on T_{ODT} was not found. A simple scaling rule, $T_{ODT} \approx e^{-x}$, between T_{ODT} and the rod length x was given, along with an R^2 of 0.999.

In addition, the results show that the method of tuning the fluidity of the BAMO–NMMO copolymers by the soft NMMO block was very restricted because the effect of f_{NMMO} on the fluidity could emerge only in the high-temperature range. In this temperature range, the BAMO–NMMO copolymers did not form the smectic phase. Once they formed the smectic phase, the effect of the NMMO blocks was lost immediately. Moreover, for the BAMO–NMMO copolymers with x, the effect of the NMMO blocks on the fluidity was also restricted.

Finally, these results could help experimental researchers select the appropriate ratio of soft blocks and rigid BAMO block lengths for energetic copolymers based on BAMO when they are used as binders of solid propellants that need appropriate melting temperature ranges.

ACKNOWLEDGMENTS

All of the authors express their gratitude for financial support from the Foundation of Chinese Academy of Engineering Physics (contract grant numbers 2012B0302037 and 2010A03002) and the National Nature Sciences Foundation of China (contract grant number 51173173). The authors also thank the editors and reviewers for their effective work.

REFERENCES

1. Provatas, A. DSTO-TR-0966; Defence Science & Technology Organization: Melbourne, Australia, **2000**.
2. Manser, G. E.; Fletcher, R. W.; Shaw, G. C. ONR Report N0014–82-C-0800; Morton Thiokol: Brigham City, UT, **1985**.
3. Luo, Y. J.; Guo, K. *Propel. Explos. Pyrotech.* **2008**, *33*, 365.
4. Sanderson, A. J.; Edwards, W. W. U.S. Pat. 6,815,522 (**2004**).
5. Sanderson, A. J.; Edwards, W. W. U.S. Pat. 6,997,997 (**2006**).
6. Pisharath, S.; Ang, H. G. *Polym. Degrad. Stab.* **2007**, *92*, 1365.
7. Kawamoto, A. M.; Holanda, J. A. S.; Barbieri, U.; Polacco, G.; Keicher, T.; Krause, H.; Kaiser, M. *Propel. Explos. Pyrotech.* **2008**, *33*, 365.
8. Talukder, M. A. H.; Lindsay, G. A. *J. Polym. Sci. Part A: Polym. Chem.* **1990**, *8*, 93.
9. Xu, B. P.; Lin, Y. C.; Chien, J. C. W. *J. Appl. Polym. Sci.* **1992**, *46*, 1603.
10. Lee, M.; Cho, B.; Kim, H.; Yoon, J.; Zin, W. *J. Am. Chem. Soc.* **1998**, *120*, 9168.
11. Lee, M.; Cho, B.; Jang, Y.; Zin, W. *J. Am. Chem. Soc.* **2000**, *122*, 7449.
12. Matsen, M. W.; Barrett, C. *J. Chem. Phys.* **1998**, *109*, 4108.
13. Al Sunaidi, A.; den Otter, W. K.; Clarke, J. H. R. *Philos. Trans. R. Soc. London A* **2004**, *362*, 1773.
14. Al Sunaidi, A.; den Otter, W. K.; Clarke, J. H. R. *J. Chem. Phys.* **2009**, *130*, 124910.
15. Wang, Q. F.; Keffer, D. J.; Nicholson, D. M. *J. Chem. Phys.* **2011**, *135*, 214903.
16. Wang, Q. F.; Keffer, D. J.; Nicholson, D. M.; Thomas, J. B. *Macromolecules* **2010**, *43*, 10722.
17. Horsch, M. A.; Zhang, Z. L.; Glotzer, S. C. *Soft Matter* **2010**, *6*, 945.
18. Lintuvuori, J. S.; Wilson, M. R. *Phys. Chem. Chem. Phys.* **2009**, *11*, 2116.
19. Wang, Q. *Soft Matter* **2011**, *7*, 3711.
20. Chou, S. H.; Wu, D. T.; Tsao, H. K.; Sheng, Y. *J. Soft Matter* **2011**, *7*, 9119.
21. Zhou, Y.; Long, X. P.; Zeng, Q. X. *J. Appl. Polym. Sci.* **2012**, *125*, 1530.
22. Zhou, Y.; Long, X. P.; Zeng, Q. X. *J. Appl. Polym. Sci.* **2012**. DOI: 10.1002/app.38482.
23. Zhou, Y.; Long, X. P.; Zeng, Q. X. *Mol. Simul.* **2012**, *38*, 961.
24. Zhou, Y.; Long, X. P.; Zeng, Q. X. *Polymer* **2011**, *52*, 6110.
25. Hoogerbrugge, P. J.; Koelman, J. M. V. *Europhys. Lett.* **1992**, *19*, 155.
26. Groot, R. D.; Warren, P. B. *J. Chem. Phys.* **1997**, *107*, 4423.
27. Espanol, P.; Warren, P. B. *Europhys. Lett.* **1995**, *30*, 191.
28. Chou, S. H.; Tsao, H. K.; Sheng, Y. J. *J. Chem. Phys.* **2011**, *134*, 034904.
29. Wilson, M. R.; Thomas, A. B.; Dennisonb, M.; Masters, A. *J. Soft Matter* **2009**, *5*, 363.